Dislocation-θ′ (Al_2Cu) Interactions during Creep Deformation of an Al-Cu Alloy

Brian Milligan[1,2] Dong Ma[2,3], Lawrence Allard[2], Amy Clarke[1], and Amit Shyam[2]

[1]Colorado School of Mines, Golden, CO, USA

[2]Oak Ridge National Laboratory, Oak Ridge, TN, USA

[3]Songshan Lake Materials Laboratory, Dongguan, China

Abstract

While precipitate-dislocation interactions are well-understood for Al-Cu alloys in tension, creep behavior has seen far less study. New, thermally-stabilized Al-Cu alloys have θ′ (Al_2Cu) as strengthening precipitates that remain stable up to 300°C (~60% of the melting temperature) and higher, where creep becomes essential to the mechanical behavior. This investigation identifies the precipitate-dislocation interactions in such an Al-Cu alloy using in-situ neutron diffraction and scanning transmission electron microscopy. Significant load transfer to the θ′ precipitates occurs, which can be attributed to dislocation loops on the interfaces of θ′ and the Al matrix. Thus, Orowan looping is identified to be the primary activity for precipitate-dislocation interactions. As Orowan looping and load transfer are associated with significant strain hardening, these results explain the excellent creep resistance seen in this alloy, and provide insights into the design of precipitation strengthened alloys with superior creep performance.

Main Text

Al-Cu alloys have a long history in numerous applications [1–3] and interest in their mechanical properties and corresponding precipitate-dislocation interaction mechanisms is widespread. The precipitate-dislocation interactions in Al-Cu alloys during monotonic tensile deformation have been extensively reported [4–9]. The fundamental precipitate-dislocation interaction mechanisms during creep deformation of Al-Cu alloys are largely unknown. A newly developed class of Al-Cu alloys with Mn and Zr additions (called ACMZ alloys) have shown thermal stability of the strengthening θ′ precipitates above 300°C [3] (~60% of the melting temperature of the alloy), where creep deformation becomes significant. Other investigators have reported that Fe and Sc addition increases the thermal stability of θ′ precipitate strengthened microstructures along with their corresponding creep resistance [10]. In the present study, we identify the mechanism by which the θ′ (Al_2Cu) strengthening phase improves the creep resistance of a highly creep resistant ACMZ alloy with Ni additions called RR350.

A relevant concept when discussing precipitate-dislocation interactions is load transfer. Load transfer can occur during plastic deformation when a high strength precipitate is bypassed by dislocations, i.e. plastic deformation occurs in the matrix, while elastic deformation occurs in the precipitate [11]. Load transfer can provide enhanced strain hardening in Al-Cu alloys through a mechanism known as backstress hardening [12]. Load transfer relies on bypass of dislocations, and will diminish when precipitates are sheared by dislocations, so the transfer of load from the matrix to the precipitates can provide a signature of the precipitate-dislocation interactions. The method to identify precipitate-dislocation interactions in Al-Cu alloys as a function of precipitate size, type, and morphology, as well as temperature, has been reported previously [13,14]. It was observed that θ′ precipitates are bypassed by dislocations in the initial stage of plastic deformation, but can be cut by dislocations later in the plastic regime *via* the delayed shearing mechanism at elevated temperature [8,9,15]. Load transfer can also

occur during creep deformation, and has been discussed for aluminum metal matrix composites [16–18], but has not been studied in precipitation strengthened aluminum alloys.

Creep deformation generally occurs in three stages [19]: primary (or transient) creep, where the creep rate is decreasing as a function of time due to strain hardening; secondary (or steady-state) creep, where the rate of strain hardening and recovery balance each other, and the strain rate is constant as a function of time; and tertiary creep, where instability occurs due to necking or void formation and strain rate increases as a function of time until rupture. Steady state creep occupies the largest fraction of creep life for most materials, and the corresponding rate is applied to identify the dominant creep mechanism.

The authors have previously studied the creep behavior in several Al-Cu alloys using traditional stress-jump creep tests, and found that the presence of θ′ precipitates improves the steady-state creep rate [20]. In addition, the presence of grain boundary precipitates further reduced the diffusion creep rate for one Al-Cu-Ni alloy called RR350. It was concluded that the θ′ precipitates prevent deformation in the grain bulk, causing deformation to occur at the grain boundaries, and the grain boundary Al-Cu-Ni precipitates slow the grain boundary mediated deformation, particularly at low stresses.

The RR350 Al-Cu-Ni alloy was further investigated in the present investigation. This alloy was chosen due to its exceptional precipitate stability at elevated temperature [3] and good creep resistance [20]. Its composition is shown in Table 1. The alloy was heat treated to a peak aged (T6) condition, then 'preconditioned' at the testing temperature to generate a thermally stable microstructure during the creep test. Details of the heat treatment are shown in Table 2.

Table 1: Composition of Alloy RR350, wt.%.

Cu	**Mn**	**Zr**	**Si**	**Zn**	**Fe**	**Ni**	**Co**	**Ti**	**Sb**	**Al**
4.8	0.19	0.17	0.05	0.01	0.09	1.2	0.26	0.21	0.17	bal.

Table 2: Heat treatments applied to the alloy prior to testing.

Step	Solutionize	Quench	Age	Precondition
Time and Temperature	535°C for 5h	80-90°C for >1h	220°C for 4h	300°C for 200h

Figure 1 displays Scanning Transmission Electron Microscopy (STEM)-High Angle Annular Dark Field (HAADF) images of the alloy in the as-aged state, and after preconditioning at 300°C for 200 h (see Table 2). Note that there is limited coarsening or transformation, even after extended high temperature exposure (the mean precipitate thickness increased by only 5.2% after the preconditioning treatment [3]).

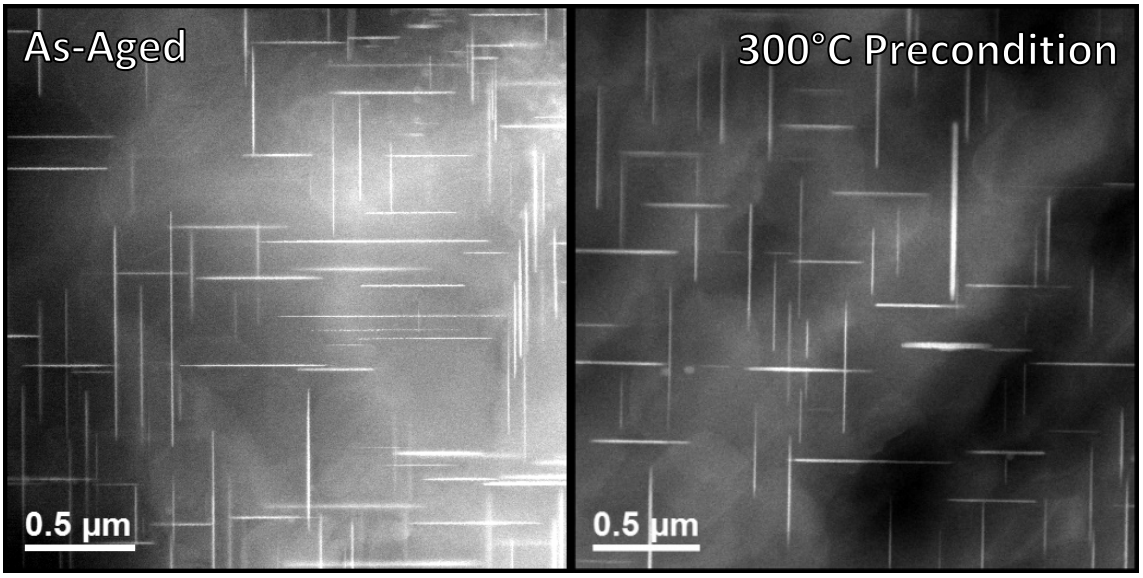

Figure 1: As-aged and 300°C preconditioned STEM images of RR350 alloy. Note that limited coarsening and transformation occurs during the preconditioning treatment, making this condition suitable for subsequent creep testing .

Two types of characterization experiments were carried out to study the precipitate-dislocation interactions during creep: in-situ neutron diffraction and ex-situ STEM. The in-situ neutron diffraction experiments were done during a creep test that utilized a Materials Testing Systems load frame with a high temperature extensometer to apply and measure stress-strain behavior; induction heating coils and two thermocouples were welded to the specimen to control temperature. Neutron data were collected continuously during the experiment from two banks of detectors aligned with diffraction vectors parallel and perpendicular to the tensile loading direction, respectively. Only the parallel bank aligned with the tensile loading direction will be discussed here for simplicity. The primary result from the neutron diffraction that will be discussed is the lattice strain ϵ_{hkl}; defined by the equation:

$$\epsilon_{hkl} = \frac{d^{hkl} - d_0^{hkl}}{d_0^{hkl}} \quad (1)$$

where d^{hkl} is the lattice interplanar spacing and d_0^{hkl} is a reference lattice interplanar spacing collected with a very small load (100 N/0.03 MPa) applied.

The creep tests were performed in-situ with multiple loads applied to each specimen to identify rate controlling deformation mechanisms. The stresses and hold times for each of these steps are shown in Table 3. Neutron diffraction data were collected continuously during the creep test, and was later chopped into 30-min segments overlapping with adjacent sections by 10 min on either side to collect sufficient neutron counts to quantify precipitate lattice strains. Stress levels were fit separately from one another, so no diffraction data was presented that overlapped multiple stress levels. As shown in Table 3, the stress was held at 80 MPa for longer duration than at the other stresses, in order to study the effect of extended secondary creep.

Table 3: Stresses and hold times for the in-situ creep test at 300 °C.

Stress (MPa)	Time (h)
80	13
85	1
90	1
95	1
100	1
105	1

A primary and secondary creep regime was observed for each of the stresses tested. Due to the high stresses, the primary regime was very short [21], so a steady-state creep rate was measurable in each of the stress conditions by a linear fit of the secondary regime. These steady state creep rates are plotted against stress in **Figure 2** to study the rate-controlling creep mechanism. There was a linear relationship between strain rate and stress on log scales, meaning that a power law relationship is followed. The slope of this line is 12.6, which is associated with the power-law breakdown creep regime [22].

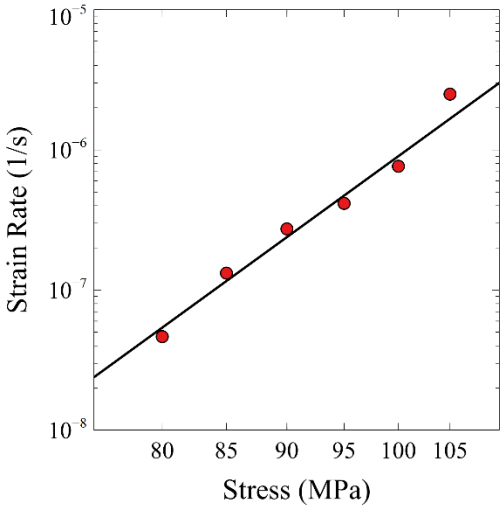

Figure 2: Minimum creep strain rates versus stresses for the RR350 alloy multiple stress creep test at 300°C. The creep exponent of 12.6 indicates the alloy is in the power-law breakdown regime [22].

The creep strain rate results are consistent with the previously-studied ex-situ creep properties at lower stresses for the RR350 alloy [20]. The in-situ neutron diffraction results provide additional information, as displayed in **Figure 3**. Note that the lattice strain in the θ′ (211) is increasing, while the lattice strains in the matrix (α (111) and α (200)) are decreasing with accumulated creep macrostrain after ~1% macrostrain (measured with extensometer). This observation is indicative of load transfer occurring during creep deformation, as the matrix and precipitate lattice stresses are departing from the bulk measurement. Also note that this load transfer behavior is monotonically increasing in a near-linear fashion as a function of macrostrain for the majority of the experiment, meaning that the load transfer mechanism is not directly dependent on stress, as the stress was varied five times during the course of

the experiment. In addition, no distinction can be seen in the load transfer behavior between the extended time creep hold at 80 MPa and the shorter holds at higher stress, even though the steady state strain rate increases by two orders of magnitude, so the load transfer mechanism is also not directly dependent on time. Therefore, the load transfer mechanism (and by extension, the precipitate-dislocation interaction mechanism) must only be directly dependent on accumulated creep strain, not on time or stress.

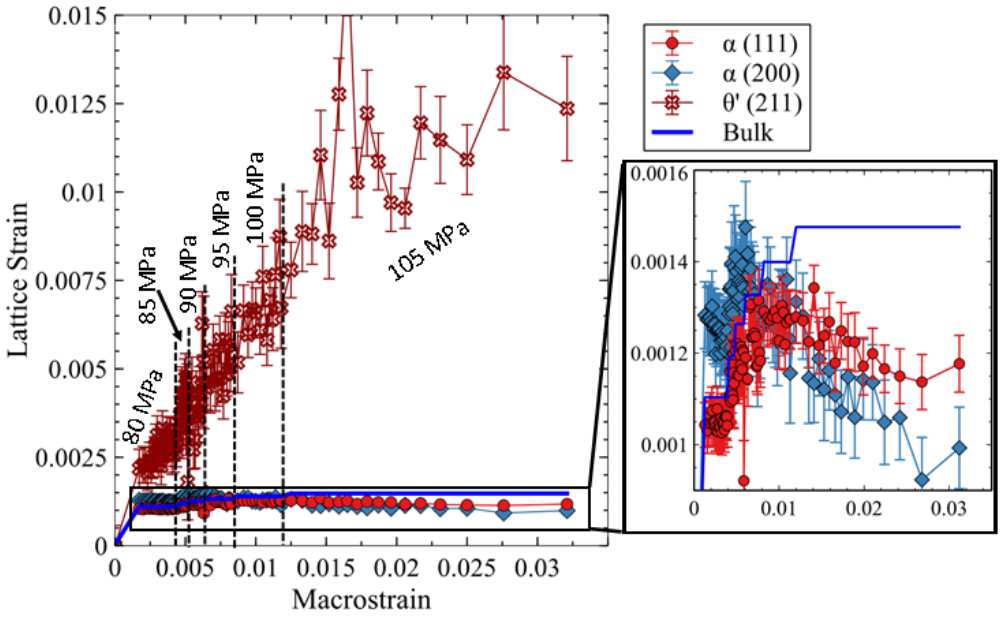

Figure 3: Lattice strain versus true strain curves for the θ′ (211) crystallographic orientation, as well as the two extremes of matrix crystallographic grain orientations. Note that the precipitate stresses are increasing over the course of the experiment, while the matrix stresses are decreasing, signifying load transfer. This degree of load transfer suggests that the primary precipitate-dislocation interaction is bypass via Orowan looping. Additional details of the same lattice strain-true strain behavior at the lower stress levels for individual crystallographic orientations can be seen in **Figure S1**.

The behavior observed here is similar to the tensile behavior of this same RR350 alloy at 300°C [14]. The primary precipitate-dislocation interactions that occurs during tensile loading is Orowan looping, followed by delayed shearing. The load transfer occurred consistently throughout the creep test, so we hypothesize that Orowan looping is the primary precipitate bypass mechanism during creep deformation. Orowan looping mechanism is consistent with prior observations, as it is only directly dependent on accumulated plastic strain (although the accumulated plastic strain may be dependent on time or stress). Orowan looping has been observed previously during creep deformation in Ni-based superalloys [23]. Also of note in Figure 3 is the anisotropy of the α phase lattice strain evolution, where the (200) crystallographic orientation is decreasing in lattice strain much faster than the (111) orientation, far more than what would be expected from anisotropic elastic properties [24]. This anisotropy is similar to the crystallographic anisotropy in strain hardening behavior during tensile testing of Al-Cu alloys, which is caused by anisotropy in load transfer. The mechanism by which this anisotropic load transfer occurs is described in detail elsewhere [13,14].

Another possible mechanism of bypass of dislocations during creep is climb. Climb as a bypass mechanism normally occurs around small precipitates [25,26]. While the precipitates in our experiments are thin, they have very high aspect ratio, and diameters greater than 350 nm. The rate of climb follows the relationship [27]:

$$\dot{v} = \frac{N_0 D \sigma b^5}{kT} \tag{2}$$

where $\dot{v}$ is the rate of climb, N_0 is the equilibrium concentration of vacancies, where $N_0 = \exp\left(\frac{E_v^f}{kT}\right)$, D is the self-diffusion coefficient, σ is the applied stress, b is the Burgers vector, k is Boltzmann's constant, T is temperature, and E_v^f is the formation enthalpy for a single vacancy. The diffusivity values were assumed here to be the same as pure aluminum [28], and E_v^f was measured using nuclear magnetic resonance [29]. Assuming the distance the dislocation must climb is half the diameter of the precipitate (D=390 nm [3]), this model predicts it will take 10^{12} s to overcome a single precipitate at 80 MPa applied stress. Climb as the primary precipitate bypass mechanism can be reasonably ruled out.

As confirmation that Orowan looping is occurring, post-mortem STEM was performed on the creep tested specimens to observe dislocations on the interfaces of the precipitates. As Figure 4 demonstrates, a multitude of Orowan loops can be observed in the STEM images for the face-on precipitates.

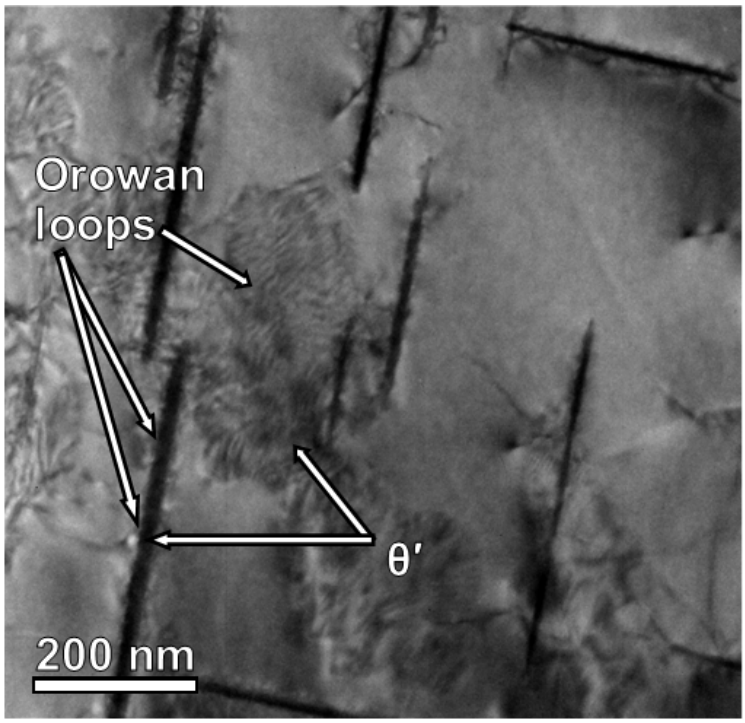

Figure 4: Post-mortem bright field STEM of the RR350 specimen creep tested at 300°C. Note the presence of dislocations on the interfaces of the θ' precipitates, which are Orowan loops. Zone axis is <200>.

There is an additional possibility that climb is occurring in the Orowan loops themselves; this mechanism has been discussed elsewhere [30]. There are two pieces of evidence refuting this mechanism

controlling the behavior, including: 1) the precipitates continue experiencing extensive load transfer, which would be reduced by climb of Orowan loops, and 2) dislocation loops can still be observed post-mortem on the interfaces of the precipitate. It was found that Orowan loops at the equator of spherical particles do not climb as they are in a metastable state, where the interface is perpendicular to the climb direction, not providing a driving force for climb [30]. We hypothesize that dislocations around θ' precipitates act similarly, where the majority of the dislocation contacts the coherent interface, which is again perpendicular to the direction of climb, thereby greatly decreasing the driving force for Orowan loop climb. The above results and discussion allow us to conclude that climb of Orowan loops is not a controlling mechanism in the behavior of these alloys at 300°C. Climb does have a strong relationship with temperature, while Orowan looping does not, so climb of Orowan loops may become an important mechanism at higher temperature and higher deformation levels when precipitates rotate around their crystallographic axes [30].

Another deformation mechanism that is possible in these alloys is cutting or shearing of the precipitates. Dislocation cutting was observed in-situ during tension in the RR350 alloy at 300°C [14], and dislocation cutting has been observed during creep in Ni-based superalloys [23]. The lattice strains reached in these experiments are comparable or higher than those reached in the tensile tests [14], but the lattice strain was not observed to increase monotonically in the monotonic tensile testing conditions. This lack of yield in the precipitates during the creep test is likely caused by the homogeneity in deformation or the extensive degree of recovery that occurs during a creep test. Inhomogeneous deformation will cause some precipitates to be cut prematurely, but such an effect is less likely to occur during a creep test.

There are significant implications to the reported deformation mechanisms. As discussed previously, steady state creep occurs when the rate of strain hardening is matched by the rate of recovery. In these alloys, a salient strain hardening mechanism is backstress hardening, which is strain hardening caused by load transfer from the matrix to the precipitate and the resulting buildup of dislocations at the interfaces. This load transfer occurs mostly as a function of macrostrain of the bulk, as seen in **Figure 3**, while recovery occurs as a function of time, temperature, and dislocation density. The steady state creep rate is then determined by the balance of these two mechanisms. Backstress hardening accounts for a large portion of strain hardening in Al-Cu alloys [15]. Backstress hardening, therefore, explains the high creep resistance observed when θ' precipitate rich microstructures are present in Al-Cu alloys [10,20]. In addition, the activation of alternative precipitate-dislocation interactions such as climb of Orowan loops or precipitate cutting would have a measurably negative effect on the creep resistance in θ' strengthened alloys. Note that none of these observations must be specific to θ' or Al-Cu alloys, and similar deformation mechanisms may occur in other alloy systems. Specifically designing precipitate structures in order to promote Orowan looping and load transfer may be a path to creating new alloys with excellent creep properties.

In summary, neutron diffraction was used to study the precipitate-dislocation interactions in a thermally-stable Al-Cu alloy RR350 with outstanding creep resistance, and the following conclusions were drawn:

- Load transfer was observed from the matrix to the precipitate during the entire creep test. The load transfer was observed to occur as a linear function of accumulated creep strain, irrespective of stress or strain rate.

- The similarity in load transfer mechanism between creep and tensile tests, as well as post-mortem STEM, identified the primary precipitate-dislocation interaction during the creep test to be Orowan looping. These Orowan loops can climb and annihilate after they are formed, but this mechanism was not found to be rate-controlling.
- We hypothesize that the balance of strain hardening versus recovery is controlled by the load transfer behavior, which explains the excellent creep resistance observed in θ′ strengthened Al-Cu alloys.

Acknowledgements

Research was supported by the Center for Advanced Non-Ferrous Structural Alloys (CANFSA), a National Science Foundation Industry/University Cooperative Research Center (I/UCRC) [Award No. 1624836], at the Colorado School of Mines (Mines). Support was also provided from the Office of Graduate Studies at Mines and the GO! Program at Oak Ridge National Laboratory (ORNL). Research at the ORNL was supported by the U.S. Department of Energy, Office of Energy Efficiency and Renewable Energy, Vehicle Technologies Office, Propulsion Materials Program. Early research was supported by the U.S. Department of Energy, Laboratory Directed Research and Development program at ORNL. A portion of this research used resources at Oak Ridge National Laboratory's Spallation Neutron Source, sponsored by the Scientific User Facilities Division, Office of Basic Energy Sciences, U.S. Department of Energy. We acknowledge David Dunand (Northwestern University) for discussions and Sumit Bahl (ORNL), Richard Michi (ORNL) and Connor Rietema (Mines) for reviewing the manuscript.

Supplementary Material

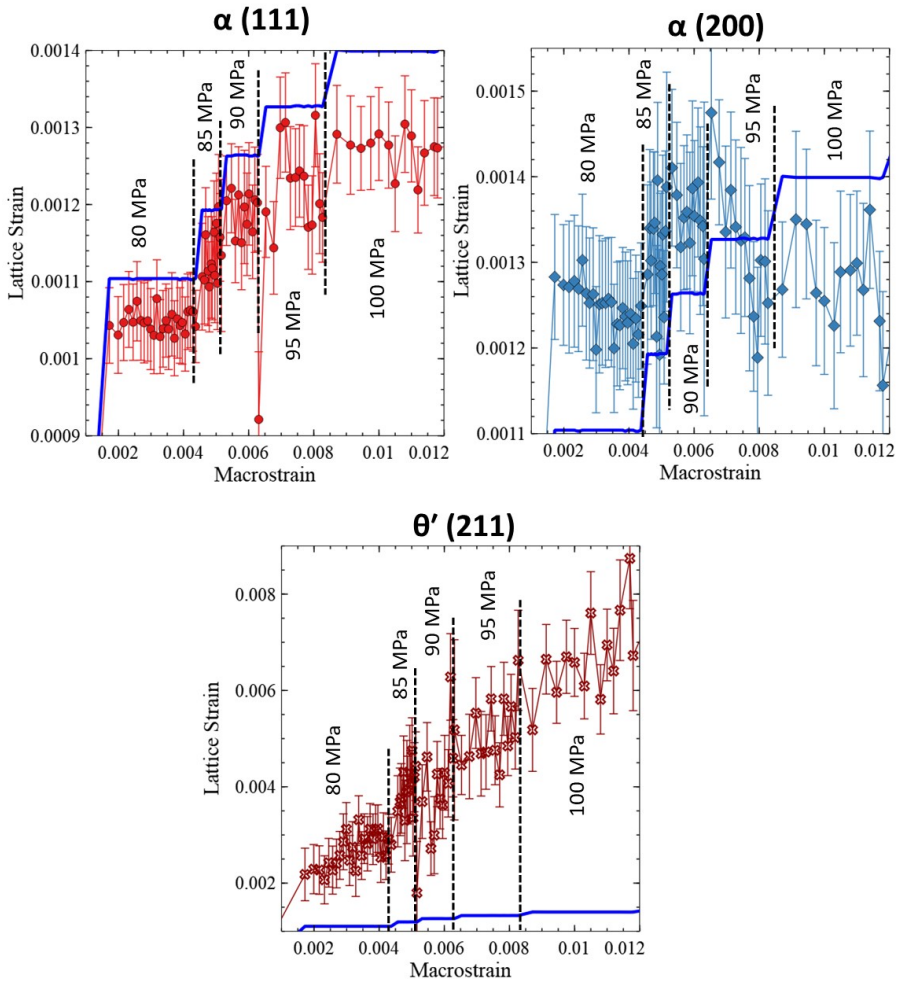

Figure S1: Detailed view of the lattice strain-macrostrain behavior of two separate orientations for the aluminum matrix and one orientation for the strengthening precipitate.

References

[1] Frank W. Gayle, Martha Goodway, Science 266 (1994) 1015–1017.
[2] David A. Porter, Kenneth E. Easterling, Mohamed Y. Sherif, in: Phase Transformations in Metals and Alloys, Third Edition, CRC Press, London, 2009, pp. 277–285.
[3] A. Shyam, S. Roy, D. Shin, J.D. Poplawsky, L.F. Allard, Y. Yamamoto, J.R. Morris, B. Mazumder, J.C. Idrobo, A. Rodriguez, T.R. Watkins, J.A. Haynes, Materials Science and Engineering: A 765 (2019) 138279.
[4] Shigeyasu Koda, Keisuke Matsuura, Susumu Takahashi, Journal of the Institute of Metals 91 (1963) 229–234.
[5] H. Liu, Y. Gao, L. Qi, Y. Wang, J.-F. Nie, Metallurgical and Materials Transactions A 46 (2015) 3287–3301.
[6] I. Adlakha, P. Garg, K.N. Solanki, Journal of Alloys and Compounds 797 (2019) 325–333.
[7] A.J. Ardell, J.C. Huang, Philosophical Magazine Letters 58 (1988) 189–197.
[8] V.S. Krasnikov, A.E. Mayer, International Journal of Plasticity 119 (2019) 21–42.

[9] C.S. Kaira, V. De Andrade, S.S. Singh, C. Kantzos, A. Kirubanandham, F. De Carlo, N. Chawla, Advanced Materials 29 (2017) 1703482.
[10] Y.H. Gao, P.F. Guan, R. Su, H.W. Chen, C. Yang, C. He, L.F. Cao, H. Song, J.Y. Zhang, X.F. Zhang, G. Liu, J.F. Nie, J. Sun, E. Ma, Materials Research Letters 8 (2020) 446–453.
[11] S. Ma, P. Rangaswamy, B.S. Majumdar, Scripta Materialia (2003) 6.
[12] J.J. Bhattacharyya, B. Bittmann, S.R. Agnew, International Journal of Plasticity (2018).
[13] B. Milligan, D. Ma, L. Allard, A. Clarke, A. Shyam, Acta Materialia 205 (2021) 116577.
[14] Brian Milligan, Sepideh Kavousi, Dong Ma, Mohsen Asle Zaeem, Amit Shyam, Amy Clarke, In Preparation (2021).
[15] J. da Costa Teixeira, L. Bourgeois, C.W. Sinclair, C.R. Hutchinson, Acta Materialia 57 (2009) 6075–6089.
[16] Y. Li, T.G. Langdon, Metall and Mat Trans A 29 (1998) 2523–2531.
[17] K.-T. Park, F.A. Mohamed, MMTA 26 (1995) 3119–3129.
[18] A.B. Pandey, R.S. Mishra, Y.R. Mahajan, Acta Metallurgica et Materialia 40 (1992) 2045–2052.
[19] G. Dieter, in: Mechanical Metallurgy, McGraw-Hill, 1988, pp. 432–470.
[20] B.K. Milligan, S. Roy, C.S. Hawkins, L.F. Allard, A. Shyam, Materials Science and Engineering: A 772 (2020) 138697.
[21] L. Esposito, Materials Science and Engineering A (2011) 6.
[22] D.R. Lesuer, C.K. Syn, O.D. Sherby, (n.d.) 16.
[23] G.B. Viswanathan, P.M. Sarosi, M.F. Henry, D.D. Whitis, W.W. Milligan, M.J. Mills, Acta Materialia 53 (2005) 3041–3057.
[24] J. Vallin, M. Mongy, K. Salama, O. Beckman, Journal of Applied Physics 35 (1964) 1825–1826.
[25] M.E. Krug, D.C. Dunand, Acta Materialia 59 (2011) 5125–5134.
[26] M.E. Krug, D.N. Seidman, D.C. Dunand, Materials Science and Engineering: A 550 (2012) 300–311.
[27] J. Weertman, Journal of Applied Physics 26 (1955) 1213–1217.
[28] T.E. Volin, R.W. Balluffi, Phys. Stat. Sol. (b) 25 (1968) 163–173.
[29] A. Seeger, D. Wolf, H. Mehrer, Phys. Stat. Sol. (b) 48 (1971) 481–496.
[30] R. Monzen, H. Mizutani, Materials Science and Engineering: A 231 (1997) 105–110.